ANALYSIS OF TEMPERATURE-DEPENDENT RESIDUAL STRESS GRADIENTS IN CMOS MICROMACHINED STRUCTURES

Hasnain Lakdawala* and Gary K. Fedder†*

Department of Electrical and Computer Engineering* and The Robotics Institute†
Carnegie Mellon University, Pittsburgh, PA 15213, USA
phone: (412) 268 4403 fax: (412) 268 3890 email: [hasnain,fedder]@ece.cmu.edu

ABSTRACT

In this paper, we present a technique to analyze variation of structural curl with temperature due to residual stress gradients in multilayer CMOS microstructures. Analytic equations verified by finite element analysis (FEA) and experiment are used as a basis for a FEA technique to predict residual stress dependent curl in an arbitrary device. A parameter extraction method based on measurement of tip deflection with temperature is proposed to extract the simulation parameters. Simple beam test structures composed of all metal-dielectric combinations possible in the Hewlett Packard 3-metal 0.5µm n-well CMOS process are experimentally characterized. This information is used to obtain the characteristic temperature at which the beam has no vertical displacement and the stresses in each layer is zero. The thermal coefficient of expansion (TCE) for each layer is extracted using the rate of change of tip deflection with temperature. The characteristic temperature and TCE are inserted in FEA for prediction of structural curl with temperature. This predictive technique has been demonstrated for a curl-matched CMOS accelerometer.

INTRODUCTION

CMOS surface-micromachining technology through conventional CMOS processing integrates circuits with mechanical structures at low cost. It provides an ability to place multiple isolated conductors in microstructures for novel capacitive sensing. The multilayer structural material, composed of metal layers with interleaved dielectric layers, exhibits residual stress gradients that induce structural curling. Stress in each layer is a function of temperature due to the differences in the TCE of the layers. This variation of structural curling leads to variation of sensitivity of lateral capacitive sensors, as the coupling area between adjacent electrodes changes. Curl-matching techniques have been used to minimize the effect of these variations[1]. To design and verify matched curl in structures it is imperative to predict structural curl variation due to temperature.

The analysis of temperature-dependent curl for CMOS micromachined beams extends Timoshenko's treatment of thermal bimorphs[2][3] and results in equations describing the beam tip deflection with temperature. The residual stress effects in each layer are represented by a characteristic temperature at which the beam is completely flat. The TCE values for each material are extracted experimentally from the measured rate of change of tip deflection with temperature. The material properties and the characteristic temperature are used in a FEA to predict curling of arbitrary CMOS surface-micromachined structures.

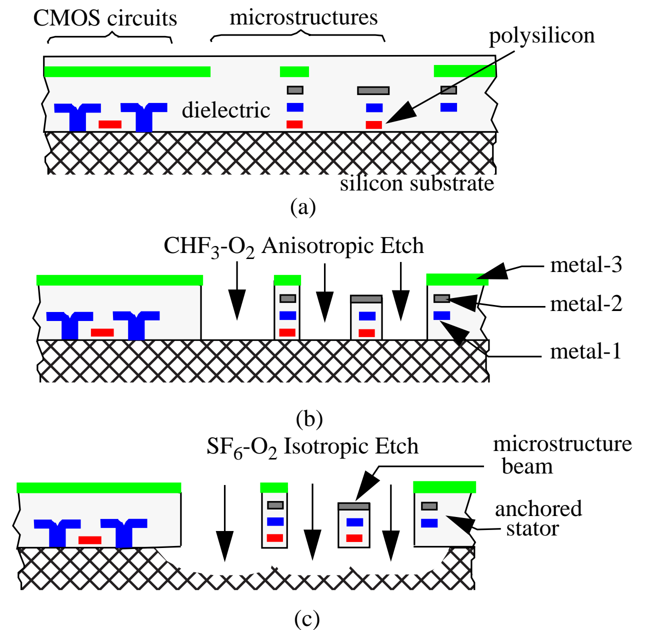

Figure 1: Schematic of the process for micromachined structures in standard CMOS.

CMOS MICROMACHINING PROCESS

The devices described in this paper have been fabricated in the high-aspect-ratio CMOS micromachining process developed at Carnegie Mellon University [4]. The process flow, shown in Figure 1, enables fabrication of micromachined structures in a standard 0.5µm 3-metal CMOS process. The conventional CMOS process is followed by an anisotropic reactive-ion etch (RIE) with CHF_3 and O_2 to etch away oxide not covered by any of the metal layers, resulting in high aspect ratio vertical sidewalls. An isotropic RIE (using SF_6 and O_2) then removes the underlying silicon, thus releasing the microstructure.

THERMAL MULTIMORPH ANALYSIS

A CMOS micromachined structure can be designed with any of the metal layers as the top metal mask leading to numerous choices for the design of each element of a device.

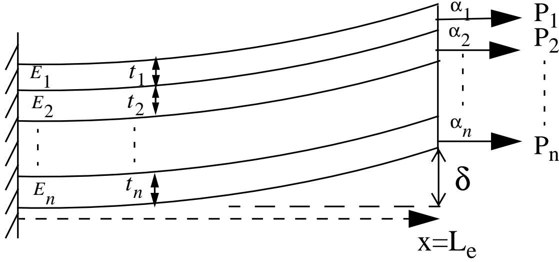

Figure 2: A CMOS cantilever beam composed of metal and dielectric layers.

The curl in each element is a function of temperature and masking metal layer. The analysis of curl with temperature for a multilayer structure is done by extending Timoshenko's analysis of thermal bimorphs[2][3]. Consider a multilayer cantilever structure shown in Figure 2 with n layers. Each layer, i, has a thickness t_i, coefficient of thermal expansion, α_i, and an effective Young's Modulus E_i. The out-of-plane curling due to residual stress gradient in the beam produces a tip deflection, δ. The material properties for each layer are assumed to be uniform throughout the layer and independent of temperature. Let P_i represent the force in each layer due to the stress.

Since no external forces are acting on the beam, the forces at the end of the beam sum to zero,

$$\sum_{i=1}^{n} P_i = 0 \tag{1}$$

The total bending moment acting on the beam is,

$$\sum_{i=1}^{n} M_i = \boldsymbol{Y}^T\boldsymbol{P} \tag{2}$$

where, $\boldsymbol{P}$ denotes the force column vector and $\boldsymbol{Y}$ is the moment arm vector,

$$\boldsymbol{P} = \begin{bmatrix} P_1 \\ P_2 \\ \dots \\ P_n \end{bmatrix}, \quad \boldsymbol{Y} = \begin{bmatrix} \frac{t_1}{2} \\ t_1 + \frac{t_2}{2} \\ \dots \\ \sum_{i=1}^{n-1} t_i + \frac{t_n}{2} \end{bmatrix} \tag{3}$$

Thickness of the beam is assumed be to much less than the radius of curvature (ρ), and the radius of curvature can be assumed to be the same for each layer.

$$\frac{1}{\rho} = \frac{M_i}{E_i I_i} \text{ or } M_i = \frac{E_i I_i}{\rho} \text{ where, } I_i = \frac{1}{12} w_i t_i^3 \tag{4}$$

where I_i is the moment of inertia of each layer having width w_i, Substituting equation (4) in (2),

$$\boldsymbol{Y}^T\boldsymbol{P} = \frac{1}{\rho}\sum_{i=1}^{n} E_i I_i = \frac{\chi}{\rho} \tag{5}$$

where, χ represents the total flexural rigidity of the beam.

The axial strain in the bottom half of the *i-th* layer is equal to that of the top half of the adjacent *(i+1)* layer. If T is the temperature, the strain in the bottom half of the upper layer is

$$\varepsilon_{l(i)} = \frac{P_i}{w_i t_i E_i} - T_0\alpha_i + T\alpha_i + \frac{t_i}{2\rho} \tag{6}$$

The strain in the top half of the lower layer is,

$$\varepsilon_{l(i+1)} = \frac{P_{i+1}}{w_{i+1} t_{i+1} E_{i+1}} - T_0\alpha_{i+1} + T\alpha_{i+1} - \frac{t_{i+1}}{2\rho} \tag{7}$$

where, T_0 denotes the characteristic temperature at which the beam has zero deflection. The term $-T_0\alpha_i$ in the above equations represents the strain due to the residual stresses. These equations are valid for low temperatures (<300°C) as the assumption that TCE is independent of temperature not accurate for higher temperatures. From equations (6) and (7),

$$\frac{P_{i+1}}{w_{i+1} t_{i+1} E_{i+1}} - \frac{P_i}{w_i t_i E_i} + (T - T_0)(\alpha_{i+1} - \alpha_i) - \frac{t_i + t_{i+1}}{2\rho} = 0 \tag{8}$$

Expressing this boundary condition for every layer interface, *n-1* equations are obtained. Expressing (1) and (8) in matrix form,

$$\boldsymbol{GP} + A(T - T_0) - \frac{1}{2\rho}\boldsymbol{S} = 0 \tag{9}$$

where, $\boldsymbol{G}$ describes the area and width affects, A and $\boldsymbol{S}$ are given by

$$\boldsymbol{G} = \begin{bmatrix} -\frac{1}{w_1 t_1 E_1} & \frac{1}{w_2 t_2 E_2} & \dots & 0 \\ 0 & -\frac{1}{w_2 t_2 E_2} & \dots & 0 \\ 0 & 0 & \dots & \frac{1}{w_i t_i E_i} \\ 1 & 1 & \dots & 1 \end{bmatrix}, \quad A = \begin{bmatrix} \alpha_2 - \alpha_1 \\ \alpha_3 - \alpha_2 \\ \dots \\ \alpha_n - \alpha_{n-1} \\ 0 \end{bmatrix} \tag{10}$$

$$\text{and} \quad \boldsymbol{S} = \begin{bmatrix} t_2 + t_1 \\ t_3 + t_2 \\ \dots \\ t_n + t_{n-1} \\ 0 \end{bmatrix} \tag{11}$$

The characteristic temperature is then computed as

$$T_0 = T - \frac{1}{2\rho}\left(\frac{2\chi - \boldsymbol{Y}^T\boldsymbol{G}^{-1}\boldsymbol{S}}{\boldsymbol{Y}^T\boldsymbol{G}^{-1}A}\right) \tag{12}$$

For small deflections, the radius of curvature is,

$$\rho = \frac{L_e^2}{2\delta} \tag{13}$$

where L_e is the length of the beam. The stress vector in each layer is expressed as function of temperature as,

$$\boldsymbol{P} = \frac{\boldsymbol{G}^{-1}\boldsymbol{S}}{2\rho} - \boldsymbol{G}^{-1}A(T_0 - T) \tag{14}$$

From (12) and (13), the tip deflection is,

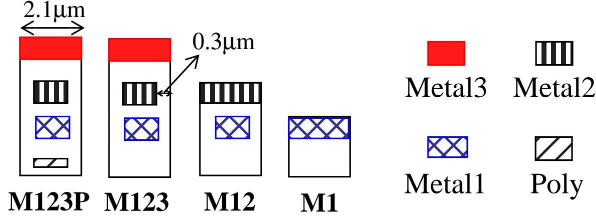

Figure 3: Example of beam combinations.

$$\delta = L_e^2(T - T_0)\left(\frac{Y^T G^{-1}}{2\chi - Y^T G^{-1} S}\right)A \tag{15}$$

Experimental Characterization

To compute the characteristic temperature and stresses in each layer using the method described above, the material properties of each layer must be known along with initial tip deflection. This is not a trivial problem as the mechanical properties of each layer depends upon the layer above and below it due to processing issues. We have extracted common material properties for each material, independent of the beam type, using parameter extraction from experimental results.

Beams having the 14 possible combinations of metal-1, metal-2, or metal-3 and polysilicon layers were fabricated. Each beam was 100µm in length, 2.1µm wide with the lower metal or polysilicon layer recessed by 0.3µm on either side. Cross sections of typical beams are shown in Figure 3.
Tip deflections were measured optically at different temperatures to 240°C. The measurement has an accuracy of +/- 0.8µm. Using (15), T_0 is extracted from a linear fit of the measure deflection over temperature. The rate of change of tip deflection with temperature is a strong function of the TCE values and is given by

$$\frac{\partial \delta}{\partial T} = L_e^2\left(\frac{Y^T G^{-1}}{2\chi - Y^T G^{-1} S}\right)A \tag{16}$$

The best fit values of the TCE of metal, dielectric and polysilicon layers are obtained. The properties used for the analysis are shown in Table 1. The best fit TCE values match closely to the values obtained from literature [5].

FINITE ELEMENT ANALYSIS

The slope for each type of beam was verified using thermomechanical FEA[6] with material properties shown in Table 1 and simulated at all measurement temperatures. The temperature boundary condition, $T_{set,}$ in the simulation is

$$T_{set} = -T_o + T_{sim} + T_d \tag{17}$$

where, T_{sim}, is the simulator initial temperature, usually 273K, and T_d is the ambient temperature. A comparison of the measured data, with analytical results and FEA is presented in Figure 4a and b. The differences in the measured tip deflection and the results from the analytical equations are within experimental error for all the cases except for metal-1 (M1), and metal-1/polysilicon (M1P) beams. This discrepancy is

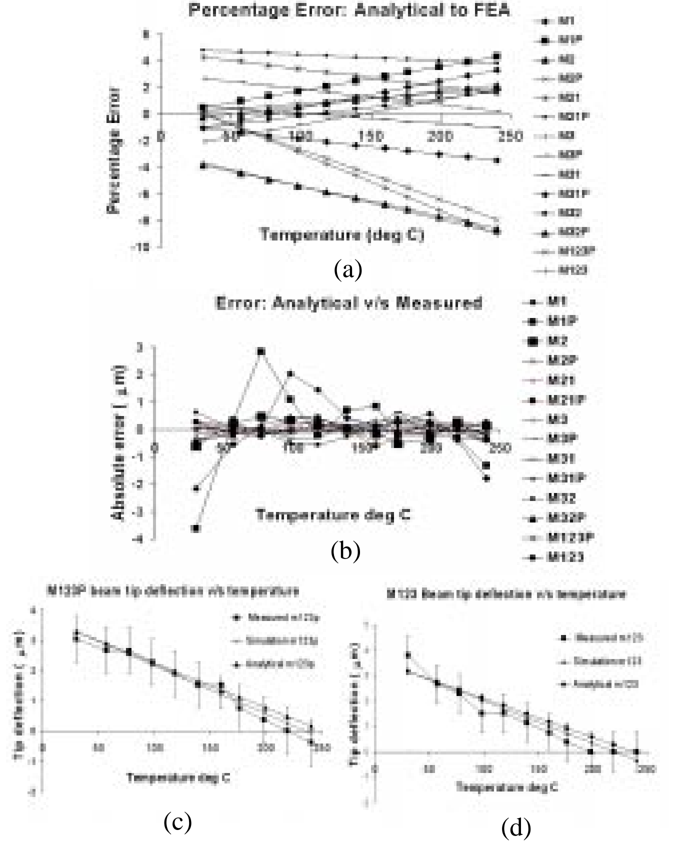

Figure 4: (a) Percentage error between experimental and FEA and Absolute error between analytical and measured data. (b) Out-of-plane tip deflection for M123 and M123P beams.

Layer	Young's Modulus	TCE
Aluminum	70 GPa	23µ
Dielectric	80 GPa	0.4µ
Polysilicon	160GPa	2.3µ

Table 1: Material properties for each layer type.

expected as the larger deflections of those beams produce non-linearities not included in the modeling. Tip deflections with temperature for beams containing metal-1, metal-2, metal-3 (M123) are shown in Figure 4c, and results for metal-1, metal-2, metal-3, polysilicon (M123P) beams are shown in Figure 4d. These beam combinations most commonly used in design. The characteristic temperature derived from the FEA for different beam combinations is listed in Table 2.

PREDICITON OF STRUCTURAL CURL

The analysis of structural curling due to residual stress gradients can be applied by using the values of material properties to general structures. A finite element model with all layers that take into account the various beam combinations of the device is automatically generated by techniques described in [7]. An example of the predictive

Beam	T_o	Beam	T_o	Beam	T_o
M123	219	**M13P**	308	**M2**	179
M123P	235	**M3**	262	**M2P**	236
M23	247	**M3P**	317	**M1**	196
M23P	248	**M12**	156	**M1P**	199
M13	243	**M12P**	119		

Table 2: Characteristic temperatures from FEA for each beam type. (*e.g.* M123P denotes a metal-1, metal-2, metal-3 and polysilicon beam.)

capability of the FEA is given by the analysis of the CMOS micromachined accelerometer[1] shown in Figure 5. To simplify assignment of temperature boundary conditions, the simulation temperature is determined by the type of beam element that dominates the accelerometer design. For the CMOS micromachined accelerometer the characteristic temperature is calculated to be 223K using a weighted average of the beam materials. This is a good approximation for this design, since one type of beam structure dominates. The simulation temperature is then computed using (17). The maximum stator deflection of the accelerometer is compared to FEA in Figure 5a. The predicted curl variation, shown in Figure 5b matches within measurement error to the curl of the actual device, as seen in Figure 5c. The close up of the curl matching between the stator and the rotor comb fingers shown in the inset.

CONCLUSIONS

Curling of multilayer microstructures must be predicted in order to design functional devices. The methodology presented here provides an accurate prediction of curl over temperature for arbitrary layouts. The analysis will result in design of reliable high performance devices in the CMOS micromachining technology. Offset and sensitivity variations over temperature in inertial sensors, such as the lateral capacitive accelerometer can be predicted and through design iteration minimized

ACKNOWLEDGEMENTS

This research effort is sponsored by the DARPA and U.S. AFRL, under agreement number F30602-97-2-0323. The authors would like to thank Microcosm Technologies for providing the MEMCAD simulation Tool and M. S. Lu for helpful discussions.

REFERENCES

[1] G. Zhang et al, “A Lateral Capacitive CMOS Accelerometer with Structural Curl Compensation”, *MEMS `99* Orlando, FL, Jan 17-21, 1999.

[2] S. Timoshenko, “Analysis of Bi-metal Thermostats”, *J. Optical Society of America*, 11, pp 233-255, 1925

[3] D. L. DeVoe, et al “Modeling and Optimal Design of Piezoelectric Cantilever Microactuators”, *J. MEMS*, vol 6, no. 3, Sept 1997

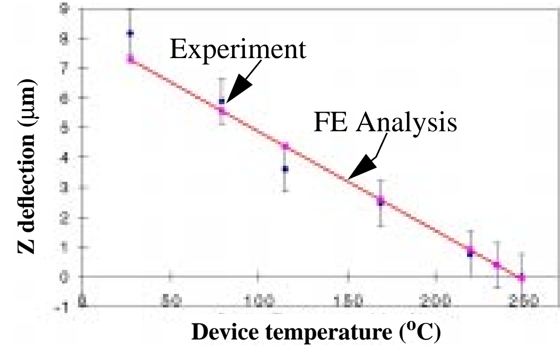

(a)

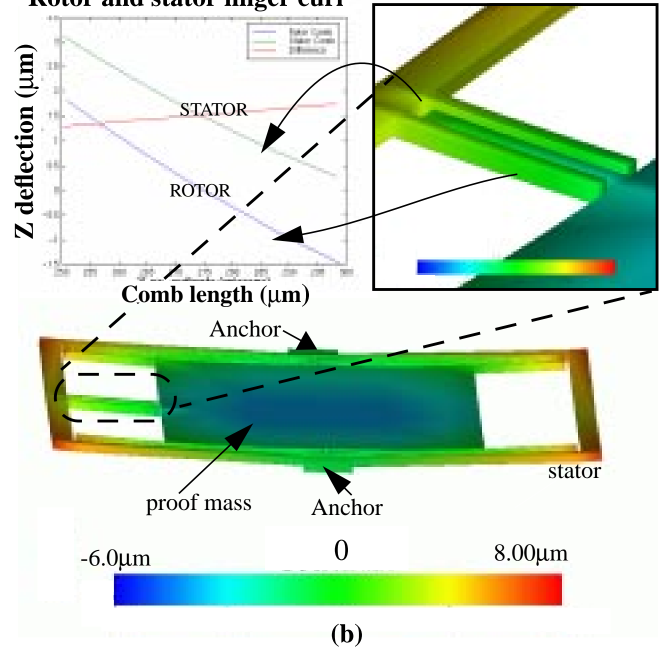

(b)

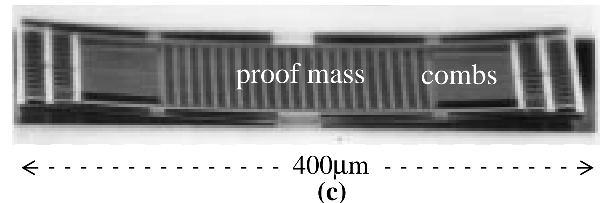

(c)

Figure 5: (a) Maximum stator deflection with temperature compared with thermomechanical FEA simulation. (b) The simulated curling in a CMOS accelerometer, (c) compared to a scanning electron micrograph of an actual device.

[4] G. K. Fedder et al, “Laminated High-Aspect-Ratio Microstructures in a Conventional CMOS Process”, *Sensors and Actuators A*, 57 pp. 103-110 1996.

[5] *MEMS material database*, http://mems.isi.edu/mems/materials/index.html

[6] *MEMCAD User Guide*, Microcosm Technologies Inc, Cary, NC 27513. http://www.memcad.com

[7] H. Lakdawala et al, “Intelligent Automatic Meshing of Multilayer CMOS Micromachined structures for Finite Element Analysis”, *Proc of MSM `99*, San Juan, Puerto Rico, April 19-21, 1999.